Brief Communication

Increase in circulating CD34-positive cells in patients with angiographic evidence of moyamoya-like vessels

Tomoyuki Yoshihara[1], Akihiko Taguchi[1], Tomohiro Matsuyama[2], Yoko Shimizu[1], Akie Kikuchi-Taura[3], Toshihiro Soma[3], David M Stern[4], Hiroo Yoshikawa[5], Yukiko Kasahara[1], Hiroshi Moriwaki[1], Kazuyuki Nagatsuka[1] and Hiroaki Naritomi[1]

[1]Department of Cerebrovascular Disease, National Cardiovascular Center, Osaka, Japan; [2]Institute for Advanced Medical Sciences, Hyogo College of Medicine, Hyogo, Japan; [3]Department of Hematology, Osaka Minami National Medical Center, Osaka, Japan; [4]Dean's Office, College of Medicine, University of Cincinnati, Cincinnati, Ohio, USA; [5]Department of Internal Medicine, Hyogo College of Medicine, Hyogo, Japan

Increasing evidence points to a role for circulating endothelial progenitor cells, including populations of CD34-positive (CD34+) cells, in maintenance of cerebral blood flow. In this study, we investigated the link between the level of circulating CD34+ cells and neovascularization at ischemic brain. Compared with control subjects, a remarkable increase of circulating CD34+ cells was observed in patients with angiographic moyamoya vessels, although no significant change was observed in patients with major cerebral artery occlusion (or severe stenosis) but without moyamoya vessels. Our results suggest that the increased level of CD34+ cells associated with ischemic stress is correlated with neovascularization at human ischemic brain.
Journal of Cerebral Blood Flow & Metabolism advance online publication, 30 January 2008; doi:10.1038/jcbfm.2008.1

Keywords: antigens; CD34; moyamoya vessel; neovascularization

Introduction

Increasing evidence points to a role for bone marrow-derived immature cells, such as endothelial progenitor cells, in maintenance of vascular homeostasis and repair. CD34-positive (CD34+) cells comprise a population enriched for endothelial progenitor cells whose contribution to neovasculature includes both direct participation in forming the neovessel and regulatory roles as sources of growth/angiogenesis factors (Majka et al, 2001). Previously, we have shown accelerated neovascularization after administration of CD34+ cells in an experimental model of stroke (Taguchi et al, 2004b) and induced by autologous bone marrow mononuclear cells (rich cell fraction of CD34+ cells) transplanted locally into patients with limb ischemia (Taguchi et al, 2003). In addition, we have observed a positive correlation between the level of circulating CD34+ cells and regional blood flow (Taguchi et al, 2004a), and cognitive function (Taguchi et al, 2007) in patients with chronic cerebral ischemia.

In this study, we have evaluated the level of circulating CD34+ cells in patients with unusually accelerated neovascularization induced by progressive occlusion (or severe stenosis) of the supraclinoid portion of the internal carotid artery, the proximal region of the anterior, and/or middle cerebral artery characterized angiographically by the presence of moyamoya-like vessels (Natori et al, 1997) that supply ischemic brain as collaterals. We have investigated the hypothesis that circulating bone marrow-derived immature cells might be associated with neovascularization at ischemic sites in the human brain.

Patients and methods

The institutional review board of the National Cardiovascular Center approved this study. All subjects provided

informed consent. A total of 50 individuals, including 24 patients with occlusion or severe stenosis (>90%) at the C1 portion of the internal carotid artery or the M1 portion of the middle cerebral artery, and 26 age-matched healthy volunteers with cardiovascular risk factors, but without history of vascular disease, were enrolled. The diagnosis of cerebral artery occlusion or stenosis was made angiographically and four patients were found to have classical angiographic evidence of moyamoya-like vessels, including one with right C1 occlusion, one with right M1 occlusion, and two with bilateral C1 severe stenosis. All patients with cerebral artery occlusion or stenosis had a history of cerebral infarction. Individuals excluded from the study included patients who experienced a vascular event within 30 days of measurements, premenopausal women, and those with evidence of infection and/or malignant disease. The number of circulating CD34+ cells was quantified as described (Taguchi et al, 2007). In brief, blood samples (200 μl) were incubated with phycoerythrin-labeled anti-CD34 antibody, fluorescein isothiocyanate-labeled anti-CD45 antibody, 7-aminoactinomycin-D (7-AAD), and internal control (all of these reagents are in the Stem-Kit; BeckmanCoulter, Marseille, France). After incubation, samples were centrifuged, and supernatant was removed to obtain concentrated cell suspensions. 7-Aminoactinomycin-D-positive dead cells and CD45-negative cells were excluded, and the number of cells forming clusters characteristic of CD34+ cells (i.e., low side scatter and low-to-intermediate CD45 staining) was counted. The absolute number of CD34+ cells was calculated using the internal control. Mean cell number of duplicate measurements was used for quantitative analysis. Statistical comparisons among groups were determined using analysis of variance or χ^2 test. Individual comparisons were performed using a two-tailed unpaired Students' t-test or Mann–Whitney's U-test. Mean ± s.e. is shown.

Results

Enrolled individuals were divided into three groups: control subjects, patients with cerebral occlusion or severe stenosis, but without the presence of vessels with angiographic characteristics of moyamoya disease, and patients with angiographic evidence of moyamoya-like vessels. Baseline characteristics of the groups are shown in Table 1. The modified Rankin scale evaluation of patients with and without moyamoya-like vessels was 0.5 ± 0.5 and 1.3 ± 0.2, respectively ($P = 0.15$). Comparing these groups, there was a significant difference in the ratio of gender and treatment with aspirin between groups. However, no significant difference was observed in the number of circulating CD34+ cells in control group between genders (male, $n = 13$, CD34+ cells = 0.93 ± 0.10/μL; female, $n = 13$, CD34+ cells = 0.85 ± 0.11/μL: $P = 0.59$) and treatment with aspirin (aspirin (+), $n = 6$, CD34+ cells = 0.76 ± 0.12/μL; aspirin (−), $n = 20$, CD34+ cells = 0.93 ± 0.09/μL: $P = 0.26$), indicating mild and nonsignificant effects of gender and treatment with aspirin on the level of circulating CD34+ cells. In univariate analysis of control subjects, each cerebrovascular risk factor and treatment with statins showed no significant difference in the number of circulating CD34+ cells (data not shown).

A representative angiogram showing characteristics of moyamoya-like vessels is shown in Figures 1A and 1B. Angiographic moyamoya-like vessels were observed around the M1 portion of an occluded middle cerebral artery. Compared with a normal subject (Figure 1C) and patients without angiographic evidence of moyamoya-like vessels (Figure 1D), a remarkable increase in levels of

Table 1 Baseline characteristics

	Total	Control	Major artery occlusion/stenosis		P-value for trend
			Moyamoya (−)	Moyamoya (+)	
N	50	26	20	4	
Age, years	60.8 ± 1.1	60.5 ± 1.9	61.5 ± 1.0	59.3 ± 5.9	0.85
Male, n (%)	33 (66)	13 (50)	18 (90)	2 (50)	0.01
Risk factor, n (%)					
Hypertension	35 (70)	16 (62)	15 (75)	4 (100)	0.24
Hyperlipidemia	26 (52)	14 (54)	10 (50)	2 (50)	0.96
Diabetes mellitus	11 (22)	7 (27)	4 (20)	0 (0)	0.46
Smoking	15 (30)	7 (27)	8 (40)	0 (0)	0.25
Treatment, n (%)					
Ca channel blockers	20 (40)	10 (38)	8 (40)	2 (50)	0.91
β-Blockers	5 (10)	3 (11)	1 (5)	1 (25)	0.44
ACE inhibitor	7 (14)	4 (15)	2 (10)	1 (25)	0.70
ARB	12 (24)	5 (19)	5 (25)	2 (50)	0.40
Diuretics	4 (8)	2 (7)	1 (5)	1 (25)	0.40
Statin therapy	14 (28)	9 (34)	4 (20)	1 (25)	0.54
Aspirin	19 (38)	6 (23)	10 (50)	3 (75)	0.05
Ticlopidine	12 (24)	3 (11)	8 (40)	1 (25)	0.08

Abbreviations: ACE, angiotensin-converting enzyme; ARB, angiotensin 2 receptor blocker.
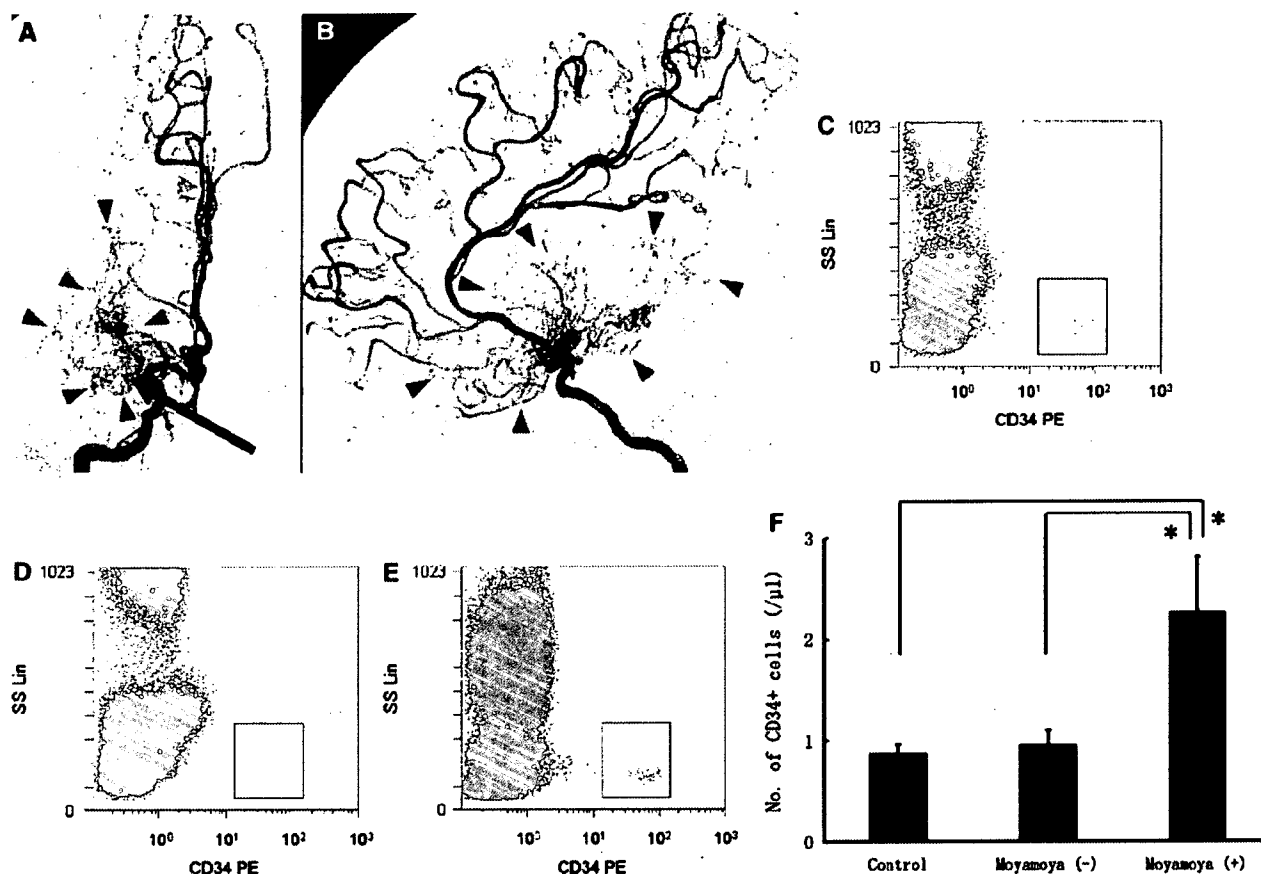
Figure 1 Increased levels of circulating CD34+ cells in patients with angiographic evidence of moyamoya-like vessels. (**A, B**) Representative angiogram from a patient with moyamoya-like vessels. Unusually accelerated neovascularization (based on angiographic features of moyamoya-like vessels, arrowheads) was observed around an occlusive M1 lesion (arrow). Anterior–posterior view (**A**) and lateral view (**B**) of the right internal carotid artery showed angiographically. (**C–E**) After exclusion of 7-aminoactinomycin-D (7-AAD)-positive dead cells and CD45-negative cells (nonleukocytes), CD34+ cells cluster at low side scatter. Representative fluorescence-activated cell sorting analyses from a control subject (**C**), a patient without moyamoya-like vessels (**D**), and a patient with moyamoya-like vessels (**E**) are shown. (**F**) A more than two-fold increase in circulating CD34+ cells was observed in patients with moyamoya-like vessels, compared with control subjects and patients without moyamoya-like vessels (*$P < 0.001$). SS Lin: side-scatter linear scale.

peripheral CD34+ cells was observed in patients with moyamoya-like vessels (Figure 1E) based on fluorescence-activated cell sorting. To confirm this impression, levels of circulating CD34+ cells were quantified (control, CD34+ cells = $0.89 \pm 0.07/\mu$L; moyamoya (−), CD34+ cells = $0.98 \pm 0.13/\mu$L; moyamoya (+), CD34+ cells = $2.28 \pm 0.53/\mu$L) and found to be significantly increased in patients with moyamoya-like vessels more than two-fold higher than in controls (Figure 1F, $P < 0.001$).

Discussion

In this study, we have found that a feature of unusually accelerated neovascularization, evidence of moyamoya-like vessels in the immediate locale of an occluded major cerebral artery, can be correlated with a robust increase in the level of circulating

CD34+ cells. The latter was determined using a newly developed method that enables quantification of few CD34+ cells in peripheral blood in a highly reproducible manner.

After acute cerebral ischemia, mobilization of CD34+ cells from bone marrow has been shown in stroke patients (Taguchi et al, 2004a). Furthermore, transplantation of CD34+ cells (Taguchi et al, 2004b) and bone marrow cells (Borlongan et al, 2004a,b) has been shown to restore cerebral blood flow in experimental models of stroke. In chronic ischemia, transplantation of CD34+ cells has also been shown to accelerate neovascularization, including formation of collateral vessels, in patients with chronic ischemic heart disease (Boyle et al, 2006) and limb ischemia (Kudo et al, 2003). In addition, there is a report regarding the correlation between inadequate coronary collateral development and reduced numbers of circulating endothelial progenitor cells in

4

patients with myocardial ischemia (Lambiase et al, 2004). In this study, we show, for the first time, a correlation between neovascularization of the cerebral arterial circulation and increased levels of circulating CD34+ cells. Our results support the hypothesis that circulating CD34+ cells potentially contribute to neovascularization at sites of ischemic brain injury.

Acknowledgements

We thank K Obata and Y Okinaka for technical assistance.

Conflict of interest

The authors state no conflict of interest.

References

Borlongan CV, Lind JG, Dillon-Carter O, Yu G, Hadman M, Cheng C, Carroll J, Hess DC (2004a) Bone marrow grafts restore cerebral blood flow and blood brain barrier in stroke rats. Brain Res 1010:108–16

Borlongan CV, Lind JG, Dillon-Carter O, Yu G, Hadman M, Cheng C, Carroll J, Hess DC (2004b) Intracerebral xenografts of mouse bone marrow cells in adult rats facilitate restoration of cerebral blood flow and blood–brain barrier. Brain Res 1009:26–33

Boyle AJ, Whitbourn R, Schlicht S, Krum H, Kocher A, Nandurkar H, Bergmann S, Daniell M, O'Day J, Skerrett D, Haylock D, Gilbert RE, Itescu S (2006) Intra-coronary high-dose CD34+ stem cells in patients with chronic ischemic heart disease: a 12-month follow-up. Int J Cardiol 109:21–7

Kudo FA, Nishibe T, Nishibe M, Yasuda K (2003) Autologous transplantation of peripheral blood endothelial progenitor cells (CD34+) for therapeutic angiogenesis in patients with critical limb ischemia. Int Angiol 22:344–8

Lambiase PD, Edwards RJ, Anthopoulos P, Rahman S, Meng YG, Bucknall CA, Redwood SR, Pearson JD, Marber MS (2004) Circulating humoral factors and endothelial progenitor cells in patients with differing coronary collateral support. Circulation 109:2986–92

Majka M, Janowska-Wieczorek A, Ratajczak J, Ehrenman K, Pietrzkowski Z, Kowalska MA, Gewirtz AM, Emerson SG, Ratajczak MZ (2001) Numerous growth factors, cytokines, and chemokines are secreted by human CD34(+) cells, myeloblasts, erythroblasts, and megakaryoblasts and regulate normal hematopoiesis in an autocrine/paracrine manner. Blood 97:3075–85

Natori Y, Ikezaki K, Matsushima T, Fukui M (1997) 'Angiographic moyamoya' its definition, classification, and therapy. Clin Neurol Neurosurg 99(Suppl 2): S168–72

Taguchi A, Matsuyama T, Moriwaki H, Hayashi T, Hayashida K, Nagatsuka K, Todo K, Mori K, Stern DM, Soma T, Naritomi H (2004a) Circulating CD34-positive cells provide an index of cerebrovascular function. Circulation 109:2972–5

Taguchi A, Matsuyama T, Nakagomi T, Shimizu Y, Fukunaga R, Tatsumi Y, Yoshikawa H, Kikuchi-Taura A, Soma T, Moriwaki H, Nagatsuka K, Stern DM, Naritomi H (2007) Circulating CD34-positive cells provide a marker of vascular risk associated with cognitive impairment. J Cereb Blood Flow Metab; e-pub ahead of print 8 August 2007

Taguchi A, Ohtani M, Soma T, Watanabe M, Kinosita N (2003) Therapeutic angiogenesis by autologous bone-marrow transplantation in a general hospital setting. Eur J Vasc Endovasc Surg 25:276–8

Taguchi A, Soma T, Tanaka H, Kanda T, Nishimura H, Yoshikawa H, Tsukamoto Y, Iso H, Fujimori Y, Stern DM, Naritomi H, Matsuyama T (2004b) Administration of CD34+ cells after stroke enhances neurogenesis via angiogenesis in a mouse model. J Clin Invest 114:330–8

Brief Communication

Circulating CD34-positive cells provide a marker of vascular risk associated with cognitive impairment

Akihiko Taguchi[1], Tomohiro Matsuyama[2], Takayuki Nakagomi[2], Yoko Shimizu[1], Ryuzo Fukunaga[3], Yoshiaki Tatsumi[4], Hiroo Yoshikawa[4], Akie Kikuchi-Taura[5], Toshihiro Soma[5], Hiroshi Moriwaki[1], Kazuyuki Nagatsuka[1], David M Stern[6] and Hiroaki Naritomi[1]

[1]Department of Cerebrovascular Disease, National Cardiovascular Center, Osaka, Japan; [2]Institute for Advanced Medical Sciences, Hyogo College of Medicine, Hyogo, Japan; [3]Department of Cerebrovascular Disease, Hoshigaoka Koseinenkin Hospital, Osaka, Japan; [4]Department of Internal Medicine, Hyogo College of Medicine, Hyogo, Japan; [5]Department of Hematology, Osaka Minami National Medical Center, Osaka, Japan; [6]Dean's Office, College of Medicine, Cincinnati University, Cincinnati, Ohio, USA

Maintenance of uninterrupted cerebral circulation is critical for neural homeostasis. The level of circulating CD34-positive (CD34⁺) cells has been suggested as an index of cerebrovascular health, although its relationship with cognitive function has not yet been defined. In a group of individuals with cognitive impairment, the level of circulating CD34⁺ cells was quantified and correlated with clinical diagnoses. Compared with normal subjects, a significant decrease in circulating CD34⁺ cells was observed in patients with vascular-type cognitive impairment, although no significant change was observed in patients with Alzheimer's-type cognitive impairment who had no evidence of cerebral ischemia. The level of cognitive impairment was inversely correlated with numbers of circulating CD34⁺ cells in patients with vascular-type cognitive impairment, but not Alzheimer's type. We propose that the level of circulating CD34⁺ cells provides a marker of vascular risk associated with cognitive impairment, and that differences in the pathobiology of Alzheimer's- and vascular-type cognitive impairment may be mirrored in levels of circulating CD34⁺ cells in these patient populations.
Journal of Cerebral Blood Flow & Metabolism (2008) **28**, 445–449; doi:10.1038/sj.jcbfm.9600541; published online 8 August 2007

Introduction

Maintaining integrity of the cerebral circulation has a critical role in neural homeostasis. Although analysis of risk factors for cerebrovascular disease has certainly provided insights into mechanisms of vascular disease, it is still difficult to predict accurately the contribution of vascular dysfunction in the long-term outcome of acute vascular insufficiency or in chronic neurodegenerative disorders. For example, in Alzheimer's disease (Casserly and Topol, 2004; Vagnucci and Li, 2003), assessment of a

possible vascular component in the pathogenesis of neuronal degeneration is often ambiguous during a patient's lifetime.

Repair of the cerebral microcirculation has traditionally been assigned to ongoing replacement of damaged cerebral endothelium from outgrowth of preexisting vasculature. However, recent studies have identified circulating bone marrow-derived immature cells, including CD34-positive (CD34⁺) cells, as contributors in maintenance of the vasculature; they have the potential to serve as a pool of endothelial progenitor cells (Asahara et al, 1997) and as a source of growth/angiogenesis factors (Majka et al, 2001). In a previous study, we have shown that circulating CD34⁺ cells provide an index of cerebrovascular function (Taguchi et al, 2004a). We have also found that in a model of experimental cerebral ischemia, intravenous administration of CD34⁺ cells improved neurologic function, at least in part, by restoring cerebral microcirculation in the ischemic area (Taguchi et al, 2004b).

Correspondence: Dr A Taguchi, Department of Cerebrovascular Disease, National Cardiovascular Center, 5-7-1 Fujishiro-dai, Suita, Osaka 565-8565, Japan.
E-mail: taguchi@ri.ncvc.go.jp

446

These results lead us to propose that circulating immature vascular progenitor cells contribute to neural homeostasis, at least in part, through their role in maintaining cerebral microvascular function. Using a recently developed method that allows precise measurement of the CD34$^+$ cell population in peripheral blood (Kikuchi-Taura et al, 2006), we have evaluated the level of circulating CD34$^+$ cells in patients with impaired neurologic function of diverse etiologies. Our goal has been to determine if there is relationship between levels of CD34$^+$ cells, impaired neural function, and vascular integrity.

Materials and methods

This study was approved by Institutional Review Boards of the respective institutions (National Cardiovascular Center, Hyogo College of Medicine, Hoshigaoka Kosei-nenkin Hospital, and Osaka Minami National Medical Center). All subjects provided informed consent. Individuals with Mini Mental State Examination Score (MMSE) < 24 and Clinical Dementia Rating (CDR) ≥ 0.5 were enrolled in this study and defined as having impaired cognitive function. In the view of history, evaluation of symptoms, and results of brain imaging studies (magnetic resonance imaging and single photon-computed tomography), patients with cognitive impairment were divided into two groups by neurologists blinded to the experimental protocol: vascular-type cognitive impairment or Alzheimer's-type cognitive impairment, according to the criteria of Diagnostic and Statistical Manual of Mental Disorders (4th ed, DSM-4) (American Psychiatric Association, 1994). To exclude the contribution of vascular element in patients with Alzheimer's-type cognitive impairment, patients' coexistent Alzheimer's-type cognitive impairment and cerebral infarction, observed by magnetic resonance imaging, were excluded from this study. In addition, patients with cognitive impairment diagnosed as neither of the Alzheimer's type nor vascular type were excluded. A total of 95 individuals, including 32 age-matched control subjects with no history of vascular disease, no neuronal deficiency, and no cognitive impairment, were enrolled. In addition, individuals excluded from the study included: premenopausal women, patients who experienced a vascular event within 30 days of measurements, history of cerebral hemorrhage, and evidence of infection or malignant disease. Using a modification of the International Society of Hematotherapy and Graft Engineering (ISHAGE) Guidelines (Sutherland et al, 1996), the number of circulating CD34$^+$ cells was quantified as described (Kikuchi-Taura et al, 2006). In brief, blood samples were incubated with phycoerythrin-labeled anti-CD34 antibody, fluorescein isothiocyanate-labeled anti-CD45 antibody, 7-aminoactinomycin-D, and internal control (all of these reagents are from the Stem-Kit, Beckman Coulter, Marseille, France). 7-Aminoactinomycin-D-positive dead cells and CD45-negative cells were excluded, and the number of cells forming a cluster with characteristic CD34$^+$ cells (i.e., low side scatter and low-to-intermediate CD45 staining) was counted. The absolute number of CD34$^+$ cells was

calculated using the internal control. In this study, we used a single measurement at the time of entry into the study, on the basis of our previous observation that the level of circulating CD34$^+$ cells is relatively stable (Taguchi et al, 2004a). For statistical analysis, JMP version 5.1J (SAS Institute Inc, Co, NC, USA) was used. Individual comparisons were performed using a two-tailed, unpaired Students' t-test. Statistical comparisons among groups were determined using analysis of variance. Mean ± s.e. is shown.

Results

Baseline characteristics of the groups are shown in Table 1. In univariate analysis of control subjects, each cerebrovascular risk factor and other treatment showed no significant difference with the number of circulating CD34$^+$ cells (data not shown).

To investigate a possible relationship between circulating CD34$^+$ cells and cognition, the level of circulating CD34$^+$ cells was compared among these groups. Representative fluorescence-activated cell sorting images are shown in Figure 1A (vascular-type) and 1B (Alzheimer's-type). Analysis of variance revealed a significant decrease of CD34$^+$ cells in patients with vascular-type cognitive impairment compared with Alzheimer's-type cognitive impairment ($P < 0.001$) and normal subjects ($P < 0.001$, Figure 1C).

To investigate further a possible association of circulating CD34$^+$ cells with cognitive impairment, patients with vascular-type impaired cognition were divided into two groups according to their CDR (mild: CDR = 0.5, $n = 22$, mean age = 75.2 ± 1.6 years; moderate-severe: CDR ≥ 1, $n = 18$, mean age = 75.3 ± 1.5 years) or MMSE (mild: MMSE ≥ 20, $n = 25$, mean age = 74.2 ± 1.4 years; moderate-severe: MMSE < 20, $n = 15$, mean age = 77.1 ± 1.5 years). The results showed a significant decrease in the level of circulating CD34$^+$ cells in moderate-severe group, based on stratification by either CDR (Figure 1D, $P = 0.01$) or MMSE (Figure 1E, $P = 0.03$) in patients with vascular-type cognitive impairment. Similar analysis was applied to patients with Alzheimer's-type impaired cognition. They were divided into two groups according to CDR (mild: $n = 8$, mean age = 73.0 ± 4.7 years; moderate-severe: $n = 15$, mean age = 77.5 ± 1.9 years) or MMSE (mild: $n = 12$, mean age = 74.1 ± 3.0 years; moderate-severe: $n = 11$, mean age = 77.8 ± 2.9 years). However, in contrast to patients with vascular-type impaired cognition, there was no significant difference observed in patients with Alzheimer's-type cognitive impaired, based on CDR (Figure 1F, $P = 0.86$) or MMSE (Figure 1G, $P = 0.60$).

Discussion

Our results are consistent with a contribution of circulating CD34$^+$ cells in support of cognitive function, presumably through their positive homeostatic influence on the cerebral circulation in

Table 1 Baseline characteristics

		Cognitive impairment			
	Total	Vascular-type	Alzheimer's-type	Control	P-value for trend
n	95	40	23	32	
Age, years	74.9±0.6	75.3±1.1	75.9±2.1	74.2±0.7	0.53
Male gender, n (%)	57 (60)	27 (68)	12 (52)	18 (56)	0.46
Risk factor, n (%)					
Hypertension	41 (43)	21 (53)	9 (39)	11 (34)	0.28
Hyperlipidemia	29 (31)	14 (35)	5 (22)	10 (31)	0.53
Diabetes mellitus	9 (9)	5 (13)	1 (4)	3 (9)	0.57
Smoking	20 (21)	10 (25)	6(26)	4 (13)	0.34
Treatment, n (%)					
Ca-channel blocker	30 (32)	15 (38)	6 (26)	9 (28)	0.56
β-Blocker	2 (2)	1 (3)	0 (0)	1 (3)	0.71
ACE inhibitor	4 (4)	3 (8)	1 (4)	0 (0)	0.29
ARB	8 (8)	3 (8)	3 (13)	2 (6)	0.65
Diuretics	6 (6)	2 (5)	1 (4)	3(9)	0.68
Statin	29 (31)	14 (35)	5 (22)	10 (31)	0.54
Aspirin	28 (29)	23 (58)	1 (4)	4 (13)	<0.01
Ticlopidine	11(12)	9 (23)	0 (0)	2 (6)	0.01

ACE, angiotensin-converting enzyme; ARB, angiotensin II receptor blocker.
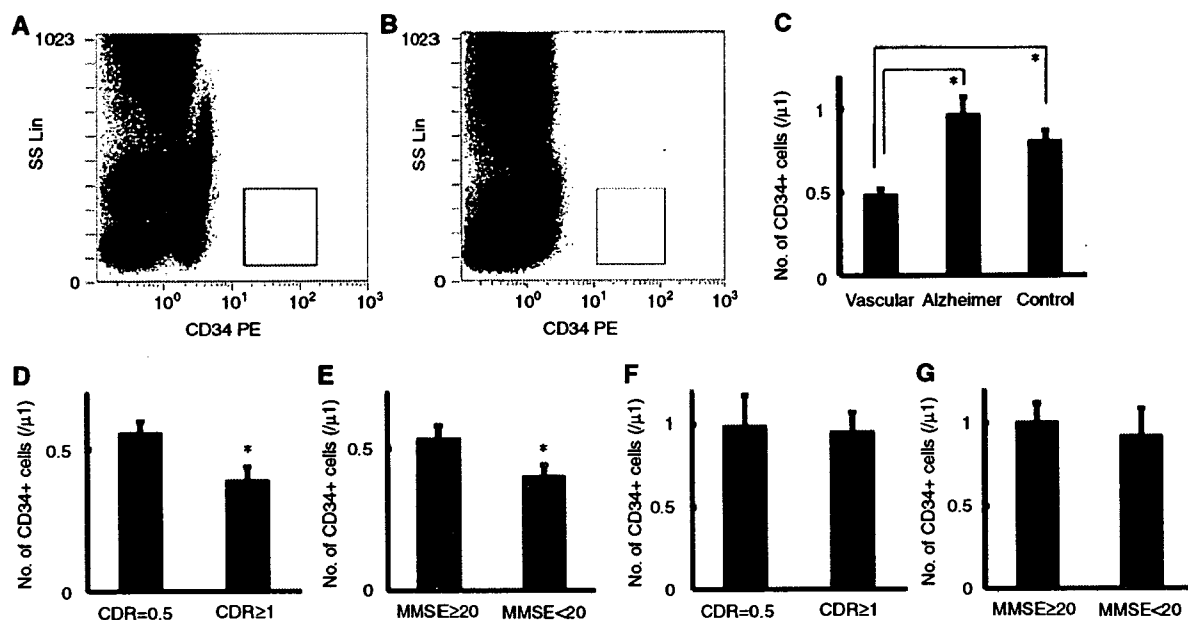
Figure 1 Levels of circulating CD34 + cells and cognitive impairment. (A and B) After exclusion of 7-AAD-positive dead cells and CD45-negative cells (non-leukocyte), CD34 + cells cluster at low side scatter were clearly observed (A, vascular-type; B, Alzheimer's-type). (C) Analysis of variance revealed a significant decrease in circulating CD34 + cells in patients with vascular-type cognitive impairment compared with normal subjects and individuals with Alzheimer's-type cognitive impairment. In contrast, no significant change in circulating CD34 + cells was observed in patients with Alzheimer's-type cognitive impairment compared with control subjects. (D and E) In the group of patients with vascular-type cognitive impairment, the level of circulating CD34 + cells was significantly reduced in patients with more severe cognitive impairment compared with the more mildly affected group (D, CDR; E, MMSE). (F and G) In contrast, no significant difference was observed in patients with Alzheimer's-type cognitive impairment based on assessment of cognition (F, CDR; G, MMSE). SS Lin, side-scatter linear scale. $*P < 0.05$.

settings of ischemic stress. Further, these observations suggest a basic difference between the pathobiology of dementia in Alzheimer's disease (without associated cerebral ischemia) and declining cognitive function in patients with ischemic cerebrovascular disorders.

448

Late onset, sporadic Alzheimer's disease is a heterogeneous disorder (Casserly and Topol, 2004) and the contribution of a vascular factor is still controversial. In contrast to vascular-type cognitive impairment, no significant change (at most, a mild increase) in the level of circulating CD34+ cells was observed in patients with Alzheimer's-type cognitive impairment who had no cerebral ischemia. Consistent with a CD34+ cell-independent mechanism of cognitive decline in Alzheimer's-type impaired cognition, there was no correlation between circulating CD34+ cells and the level of CDR or MMSE. These results suggest that the level of CD34+ cells in the peripheral circulation might provide a useful means of separating dementia with a vascular etiology from dementia associated with nonvascular causes. This is not inconsistent with a previous report indicating decreased levels of CD34+ cells in patients with early Alzheimer's disease that did not exclude patients with coexisting cerebral ischemia (Maler et al, 2006). Our findings could have implications for treatment, especially as more modalities become available for patients with declining cognitive function.

The level of circulating endothelial progenitor cells, identified based on positivity for CD34 and kinase insert domain receptor (CD34+/KDR+ cells), has been correlated with cardiovascular risk factors (Vasa et al, 2001) and cardiovascular outcomes (Schmidt-Lucke et al, 2005; Werner et al, 2005). However, large variations in the levels of CD34+/KDR+ cells in the latter reports (by ~100-fold between reports; Fadini et al, 2006; Werner et al, 2005) indicate the need to standardize this measurement. In contrast, in our study, although there was no strong correlation between levels of CD34+ cells and established cardiovascular risk factors and other treatments, probably because of the heterogeneity of our control subjects, the results indicate a close relationship between the overall CD34+ pool and the cognitive impairment with cerebral ischemia. Previous reports have indicated a positive correlation between mobilization of CD34+ cells and improved functional outcome in stroke patients (Dunac et al, 2007). Accelerated functional recovery after experimental stroke, because of administration of CD34+ cells (Shyu et al, 2006; Taguchi et al, 2004b), suggests the possible contribution of CD34+ cells in maintenance of brain function during cerebral circulation. Our method for quantification of CD34+ cells is simple, reproducible (Kikuchi-Taura et al, 2006), and suitable for screening a broad group of patients at risk for cerebrovascular disorders.

In conclusion, our results indicate that the level of circulating CD34+ cells provides a marker of vascular risk associated with cognitive impairment. Furthermore, differences in the pathobiology of Alzheimer's- and vascular-type cognitive impairment may be mirrored in levels of circulating CD34+ cells in these patient populations.

Conflict of interest

The authors state no conflict of interest.

References

American Psychiatric Association (1994) Diagnostic and statistical manual of mental disorders. 4th ed Washington, DC: American Psychiatric Association

Asahara T, Murohara T, Sullivan A, Silver M, van der Zee R, Li T, Witzenbichler B, Schatteman G, Isner JM (1997) Isolation of putative progenitor endothelial cells for angiogenesis. Science 275:964–7

Casserly I, Topol E (2004) Convergence of atherosclerosis and Alzheimer's disease: inflammation, cholesterol, and misfolded proteins. Lancet 363:1139–46

Dunac A, Frelin C, Popolo-Blondeau M, Chatel M, Mahagne MH, Philip PJ (2007) Neurological and functional recovery in human stroke are associated with peripheral blood CD34+ cell mobilization. J Neurol 254:327–32

Fadini GP, Coracina A, Baesso I, Agostini C, Tiengo A, Avogaro A, de Kreutzenberg SV (2006) Peripheral blood CD34+KDR+ endothelial progenitor cells are determinants of subclinical atherosclerosis in a middle-aged general population. Stroke 37:2277–82

Kikuchi-Taura A, Soma T, Matsuyama T, Stern DM, Taguchi A (2006) A new protocol for quantifying CD34+ cells in peripheral blood of patients with cardiovascular disease. Texas Heart Inst J 33:427–9

Majka M, Janowska-Wieczorek A, Ratajczak J, Ehrenman K, Pietrzkowski Z, Kowalska MA, Gewirtz AM, Emerson SG, Ratajczak MZ (2001) Numerous growth factors, cytokines, and chemokines are secreted by human CD34(+) cells, myeloblasts, erythroblasts, and megakaryoblasts and regulate normal hematopoiesis in an autocrine/paracrine manner. Blood 97:3075–85

Maler JM, Spitzer P, Lewczuk P, Kornhuber J, Herrmann M, Wiltfang J (2006) Decreased circulating CD34+ stem cells in early Alzheimer's disease: evidence for a deficient hematopoietic brain support? Mol Psychiatry 11:1113–5

Schmidt-Lucke C, Rossig L, Fichtlscherer S, Vasa M, Britten M, Kamper U, Dimmeler S, Zeiher AM (2005) Reduced number of circulating endothelial progenitor cells predicts future cardiovascular events: proof of concept for the clinical importance of endogenous vascular repair. Circulation 111:2981–7

Shyu WC, Lin SZ, Chiang MF, Su CY, Li H (2006) Intracerebral peripheral blood stem cell (CD34+) implantation induces neuroplasticity by enhancing beta1 integrin-mediated angiogenesis in chronic stroke rats. J Neurosci 26:3444–53

Sutherland DR, Anderson L, Keeney M, Nayar R, Chin-Yee I (1996) The ISHAGE guidelines for CD34+ cell determination by flow cytometry. International Society of Hematotherapy and Graft Engineering. J Hematother 5:213–26

Taguchi A, Matsuyama T, Moriwaki H, Hayashi T, Hayashida K, Nagatsuka K, Todo K, Mori K, Stern DM, Soma T, Naritomi H (2004a) Circulating CD34-positive cells provide an index of cerebrovascular function. *Circulation* 109:2972–5

Taguchi A, Soma T, Tanaka H, Kanda T, Nishimura H, Yoshikawa H, Tsukamoto Y, Iso H, Fujimori Y, Stern DM, Naritomi H, Matsuyama T (2004b) Administration of CD34+ cells after stroke enhances neurogenesis via angiogenesis in a mouse model. *J Clin Invest* 114: 330–8

Vagnucci Jr AH, Li WW (2003) Alzheimer's disease and angiogenesis. *Lancet* 361:605–8

Vasa M, Fichtlscherer S, Aicher A, Adler K, Urbich C, Martin H, Zeiher AM, Dimmeler S (2001) Number and migratory activity of circulating endothelial progenitor cells inversely correlate with risk factors for coronary artery disease. *Circ Res* 89:E1–7

Werner N, Kosiol S, Schiegl T, Ahlers P, Walenta K, Link A, Bohm M, Nickenig G (2005) Circulating endothelial progenitor cells and cardiovascular outcomes. *New Engl J Med* 353:999–1007

Granulocyte colony-stimulating factor has a negative effect on stroke outcome in a murine model

Akihiko Taguchi,[1] Zhongmin Wen,[1] Kazunori Myojin,[1] Tomoyuki Yoshihara,[1] Takayuki Nakagomi,[2] Daisuke Nakayama,[1] Hidekazu Tanaka,[3] Toshihiro Soma,[4] David M. Stern,[5] Hiroaki Naritomi[1] and Tomohiro Matsuyama[2]

[1]Department of Cerebrovascular Disease, National Cardiovascular Center, 5-7-1 Fujishiro-dai, Suita, Osaka, Japan, 565-8565
[2]Department of Advanced Medicine, Hyogo College of Medicine, Hyogo, Japan
[3]Department of Pharmacology, Graduate School of Medicine, Osaka University, Osaka, Japan
[4]Department of Hematology, Osaka Minami National Hospital, Osaka, Japan
[5]Dean's Office, College of Medicine, University of Cincinnati, OH, USA

Abstract

The administration of CD34-positive cells after stroke has been shown to have a beneficial effect on functional recovery by accelerating angiogenesis and neurogenesis in rodent models. Granulocyte colony-stimulating factor (G-CSF) is known to mobilize CD34-positive cells from bone marrow and has displayed neuroprotective properties after transient ischemic stress. This led us to investigate the effects of G-CSF administration after stroke in mouse. We utilized permanent ligation of the M1 distal portion of the left middle cerebral artery to develop a reproducible focal cerebral ischemia model in CB-17 mice. Animals treated with G-CSF displayed cortical atrophy and impaired behavioral function compared with controls. The negative effect of G-CSF on outcome was associated with G-CSF induction of an exaggerated inflammatory response, based on infiltration of the peri-infarction area with CD11b-positive and F4/80-positive cells. Although clinical trials with G-CSF have been started for the treatment of myocardial and limb ischemia, our results indicate that caution should be exercised in applying these results to cerebral ischemia.

Introduction

Granulocyte colony-stimulating factor (G-CSF) was identified in 1975 and has been broadly used for mobilizing granulocytes from bone marrow (Weaver *et al.*, 1993). G-CSF is also known to mobilize immature hematopoietic cells that include endothelial progenitor cells (EPCs) (Willing *et al.*, 2003). In view of the capacity of circulating EPCs to enhance neovascularization of ischemic tissues (Asahara *et al.*, 1997), the results of recent studies demonstrating that infusion of EPCs accelerates angiogenesis at ischemic sites, thereby limiting tissue injury, is not unexpected (Dzau *et al.*, 2005). As a potential extension of this concept, administration of G-CSF has been shown to accelerate angiogenesis in animal models of limb and myocardial ischemia (Minatoguchi *et al.*, 2004). These observations have provided a foundation for clinical trials testing the effects of G-CSF in limb and myocardial ischemia (Kuethe *et al.*, 2004).

Stroke, a critical ischemic disorder in which there are important opportunities for neuroprotective therapies, is another situation in which enhanced angiogenesis might be expected to improve outcome. For example, we have shown that the administration of CD34-positive cells after stroke accelerates angiogenesis and, subsequently, neurogenesis (Taguchi *et al.*, 2004). Similarly, erythropoietin (EPO), also known to have angiogenic properties, has been shown to have beneficial effects in experimental cerebral ischemia (Ehrenreich *et al.*, 2002; Wang *et al.*, 2004). In addition, G-CSF displays neuroprotective

properties *in vitro* (Schabitz *et al.*, 2003) and *in vivo* (Schabitz *et al.*, 2003; Shyu *et al.*, 2004; Gibson *et al.*, 2005), the latter in a rodent model of transient cerebral ischemic damage. Models of transient cerebral ischemia allow subtle assessment of neuroprotective properties, such as the survival of vulnerable neuronal populations in the penumbra. However, functional outcome after stroke is also determined by inflammation and reparative processes consequent to extensive brain necrosis, the latter better modelled by permanent cerebral ischemia. We have evaluated the effect of G-CSF on stroke outcome in a model of permanent cerebral ischemia with massive cell necrosis. Our model employs permanent ligation of the left middle cerebral artery (MCA) and results in extensive neuronal death in the ischemic zone, as well as more selective apoptotic cell death in the penumbral area (Walther *et al.*, 2002). Using this model, we have tested the effect of G-CSF on functional recovery after stroke.

Materials and methods

All procedures were performed under the auspices of an approved protocol of the Japanese National Cardiovascular Center Animal Care and Use Committees (protocol no. 06026, approval date, May 22, 2006).

Induction of focal cerebral ischemia

To assess the effect of G-CSF on stroke, we developed a highly reproducible murine stroke model applying our previous method

(Taguchi *et al.*, 2004) to CB-17 mice (Clea, Tokyo, Japan). Under halothane anesthesia (inhalation of 3%), the left zygoma was dissected to visualize the MCA through the cranial bone. A hole was made using a dental drill in the bone (diameter 1.5 mm) and the MCA was carefully isolated, electro-cauterized and disconnected just distal to its crossing of the olfactory tract (distal M1 portion). Cerebral blood flow in the MCA area was monitored as described previously (Matsushita *et al.*, 1998). Briefly, an acrylate column was attached to the intact skull using stereotactic coordinates (1 mm anterior and 3 mm lateral to the bregma) and cerebral blood flow was assessed using a linear probe (1 mm in diameter) by laser Doppler flowmetry (Neuroscience Co. Ltd, Osaka, Japan). Mice that showed decreased cerebral blood flow by ~75% immediately after the procedure were used for experiments (success rate of > 95%). Body temperature was maintained at 36.5–37 °C using a heat lamp (Nipponkoden, Tokyo, Japan) during the operation and for 2 h after MCA occlusion. At later timepoints, mice were first subjected to behavioral tests and then to histological examination of their brains. For histological examination, mice were perfusion-fixed with 100 mL of periodate-lysine-paraformaldehyde fixative under deep (pentobarbital) anesthesia (100 mg/kg, intraperitonealy) and their brains were removed. Coronal brain sections (20 μm) were cut on a vibratome (Leica, Solms, Germany) and subjected to immunocytochemistry.

Administration of granulocyte colony-stimulating factor and erythropoietin following stroke

To examine the effect of G-CSF on ischemic cerebral injury, human recombinant G-CSF (Kirin, Tokyo, Japan) was administered subcutaneously at four doses (0.5, 5, 50 or 250 μg/kg) at 24, 48 and 72 h after induction of stroke. As controls, the same volume of phosphate-buffered saline (PBS) or recombinant human EPO (1000 μg/kg; Kirin), the latter known to have angiogenic properties and a positive effect on stroke outcome (Jaquet *et al.*, 2002), was administered subcutaneously. Other time courses of G-CSF administration, including 1 h after stroke (at doses of 0.5, 5, 50 or 250 μg/kg) and continuous administration (100 μg/kg/day) by micro-osmotic pump (Durect, Cupertino, CA, USA) started 1 h after stroke over 7 days, were also studied. To exclude possible effects of an immune response to human recombinant G-CSF in the mouse, murine recombinant G-CSF (R & D Systems, Minneapolis, MN, USA; doses of 0.5, 5 or 50 μg/kg) was administered subcutaneously at 24, 48 and 72 h after induction of stroke, as indicated.

Immunohistochemistry

To evaluate the inflammatory response following administration of G-CSF post-stroke, brain sections were studied immunohistochemically using antibody to CD11b (BD Biosciences, San Jose, CA, USA) and F4/80 (Serotec, Raleigh, NC, USA). The numbers of CD11b-positive inflammatory cells at the anterior cerebral artery (ACA)/MCA border of the infarcted area and numbers of F4/80-positive (F4/80$^+$) activated microglia/macrophages in the ACA area at the exact center of the forebrain section (at the midpoint of the left forebrain, as shown with an orange line in Fig. 1J) were scored by two investigators blinded to the experimental protocol.

Analysis of the peri-infarction and infarcted area after middle cerebral artery occlusion

To investigate mechanisms of brain damage/atrophy consequent to administration of G-CSF, neovessel formation and the extent of infarction were analysed. Formation of new vessels was assessed at the border of the MCA and ACA territories by perfusing carbon black (0.5 mL; Fuekinori, Osaka, Japan) via the left ventricle of the heart. Staining with 2,3,5-triphenyltetrazolium (TTC) (Sigma-Aldrich, St Louis, MO, USA) was employed to demarcate the border of viable/non-viable tissue. Semiquantitative analysis of angiogenesis employed an angiographic score. Briefly, microscopic digital images were scanned into a computer (Keyence, Osaka, Japan) and the number of carbon black-positive microvessels crossing the border zone of the TTC-negative MCA area to the TTC-positive ACA area was determined. To evaluate the infarcted area 3 days after stroke, coronal brain sections at the exact center of the forebrain were stained with TTC. The infarcted area was measured using a microscopic digital camera system (Olympus, Tokyo, Japan). Infarction in this stroke model was highly reproducible and limited to the left cortex. NIH IMAGE software was used to quantify the TTC-positive area in the ACA territory. A brain atrophy index was established using whole brain images captured by a digital camera system (Olympus). The length of the forebrain was measured along the *x* and *y* dimensions shown in Fig. 1J and the ratio of *x* : *y* was defined as the brain atrophy index.

Behavioral analysis

To assess cortical function, mice were subjected to behavioral testing using the open field task (Kimble, 1968) at 35 days after stroke. In this behavioral paradigm, animals were allowed to search freely in a square acrylic box (30 × 30 cm) for 60 min. A light source on the ceiling of the enclosure was on during the first 30 min (light period) and was turned off during a subsequent 30-min period. On the X- and Y-banks of the open field, two infrared beams were mounted 2 cm above the floor, spaced at 10 cm intervals, forming a flip–flop circuit between them. The total number of beam crossings by the animal was counted and scored as traveling behavior (locomotion). Twelve infrared beams were set 5 cm above the floor, spaced at 3 cm intervals, on the X-bank and the total number of beam crossings was counted and scored as rearing behavior (rearing). To exclude the contribution of physical deficits directly related to the operative procedure and induction of stroke, motor deficiencies were examined on day 35 after stroke. Neurological deficits were scored on a three-point modified scale as described previously (Tamatani *et al.*, 2001): 0, no neurological deficit; 1, failure to extend the left forepaw fully; 2, circling to left and 3, loss of walking or righting reflex. Body weight, monitored in each experimental group, displayed no significant differences (data not shown).

Data analysis

Statistical comparisons among groups were determined using one-way ANOVA and the Dunnett test was used for post-hoc analysis to compare with PBS controls. Where indicated, individual comparisons were performed using Student's *t*-test. In all experiments, mean ± SEM is reported.

Results

Induction of stroke in CB-17 mice

In a previous report, we demonstrated reproducible strokes in severe combined immunodeficient (SCID) mice by permanent ligation of the left MCA (Taguchi *et al.*, 2004). As SCID mice originated from the CB-17 strain, we expected anatomical similarity of cerebral arteries in
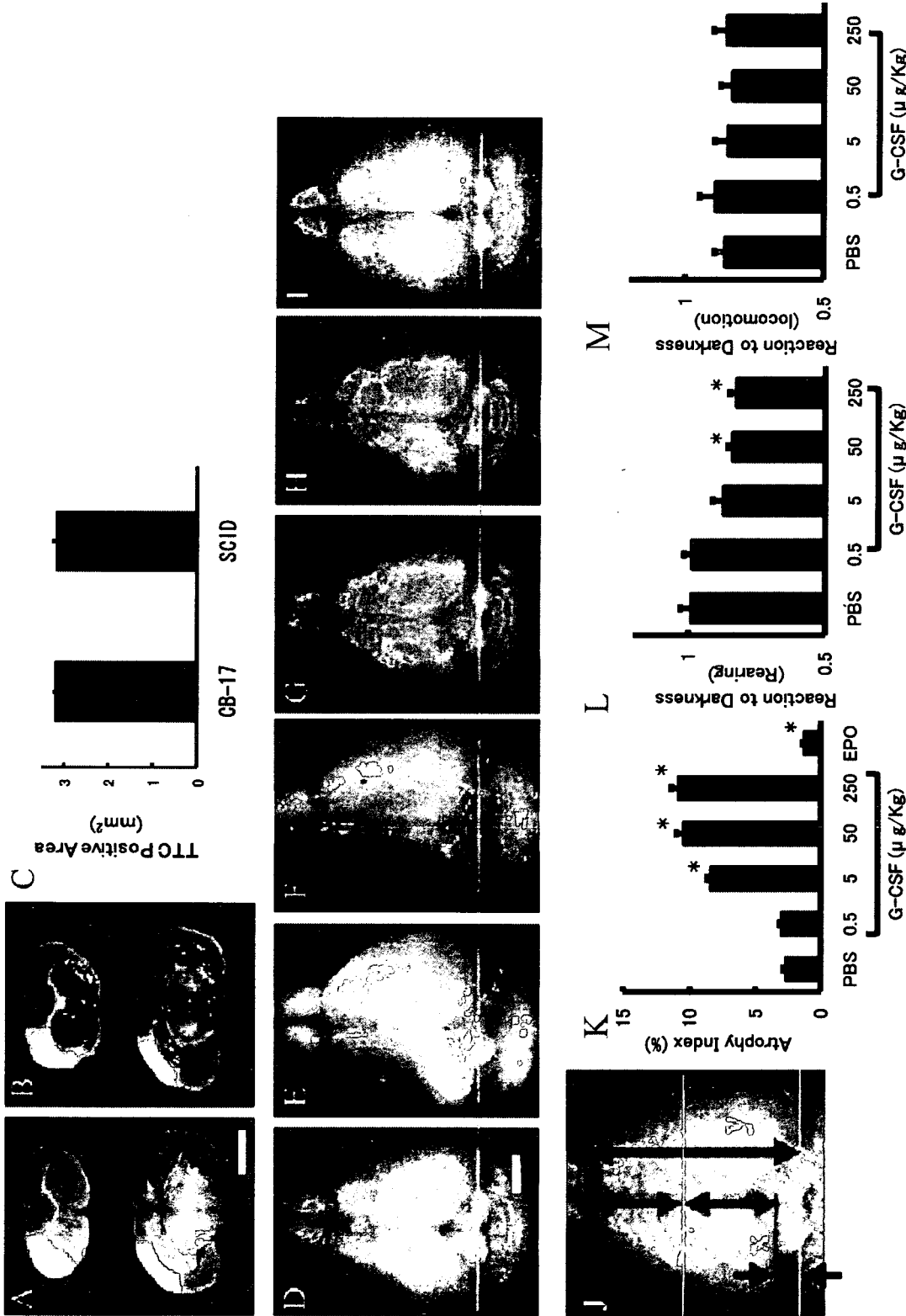
FIG. 1. Administration of granulocyte colony-stimulating factor (G-CSF) induces cortical atrophy. (A–C) Induction of stroke by ligation of the M1 portion of the left middle cerebral artery (MCA). Forebrain sections harvested from mice 3 h after stroke were stained with 2,3,5-triphenyltetrazolium (TTC), and lack of positive staining is observed in the MCA cortex of CB-17 (A) and severe combined immunodeficient (SCID) mice (B). The TTC-positive anterior cerebral artery area at the exact center of forebrain was quantified using NIH IMAGE (C). A highly reproducible TTC-positive (surviving) cortical area was observed in CB-17 and SCID mice. (D–I) On day 35 post-stroke, brains were evaluated grossly. Compared with post-stroke mice treated with phosphate-buffered saline (PBS) (D), no significant difference was observed in mice treated with 0.5 μg/kg of G-CSF (E). In contrast, brain atrophy was observed with G-CSF treatment at doses of 5 μg/kg (F), 50 μg/kg (G) or 250 μg/kg (H). Treatment with erythropoietin (EPO) (I) had a beneficial effect in terms of brain atrophy. Note that, compared with the contralateral side (green line), atrophy in the longitudinal direction was observed in animals treated with G-CSF (F–H). (J) A brain atrophy index was defined as the ratio of *x* : *y*. (K) ANOVA analysis (*n* = 6 per group) revealed significant brain atrophy in mice at doses of G-CSF above 0.5 μg/kg. In contrast, a reduction of brain atrophy was observed in mice treated with EPO. (L and M) Behavioral analysis post-stroke. ANOVA analysis (*n* = 6 per group) in mice subjected to stroke revealed that treatment with either 50 or 250 μg/kg of G-CSF significantly impaired the rearing response compared with PBS (L), although no significant difference was observed in locomotion (M). Marker bars, 2 mm (A and D). *P < 0.05 vs. PBS.

these two strains. Strokes were induced in CB-17 mice by permanent ligation of the M1 distal portion of the left MCA. To evaluate the infarcted area, brain sections were stained with TTC at 3 h after stroke. Reproducible strokes were induced in CB-17 mice (Fig. 1A) that were similar to those in SCID mice (Fig. 1B). The surviving cortical area post-stroke, represented by the TTC-positive ACA area at the exact center of forebrain, was also similar in CB-17 and SCID mice (Fig. 1C, $n = 6$/species).

Granulocyte colony-stimulating factor accelerates brain injury after stroke

In a previous study, we demonstrated that enhanced neovascularization post-stroke, due to administration of CD34-positive cells, promoted neuronal regeneration leading to cortical expansion and functional recovery (Taguchi et al., 2004). As G-CSF is known to mobilize CD34-positive cells from bone marrow (Kuethe et al., 2004), we investigated the effects of G-CSF treatment, starting 24 h after stroke and continuing for 3 days, using the above permanent focal cerebral ischemia model. Compared with control animals receiving PBS alone (Fig. 1D), no significant difference was observed in mice that received 0.5 µg/kg of G-CSF (Fig. 1E and K) at 35 days after stroke. However, remarkable brain atrophy was observed with G-CSF treatment at 5 µg/kg (Fig. 1F and K), 50 µg/kg (Fig. 1G and K) or 250 µg/kg (Fig. 1H and K). In contrast, a mild protective effect, with respect to brain atrophy, was observed in the group treated with EPO post-stroke (1000 µg/kg; Fig. 1I and K). In each condition depicted in Fig. 1, a representative image is shown and quantitative analysis of the brain atrophy index ($n = 6$/experimental condition; defined in Fig. 1J) is demonstrated in Fig. 1K.

Granulocyte colony-stimulating factor has a negative effect on functional recovery after stroke

To investigate functional recovery in animals treated with G-CSF, we performed behavioral testing on day 35 after stroke ($n = 6$, for each group). Compared with post-stroke CB-17 mice that received PBS, mice treated with 50 or 250 µg/kg G-CSF displayed impaired behavioral function as assessed by the 'dark' response, with respect to rearing (Fig. 1L and Table 1) analysed by ANOVA followed by post-hoc Dunnett test, although there was no significant change in locomotion (Fig. 1M). In contrast, treatment with EPO accelerated functional recovery with respect to both rearing (1.18 ± 0.07 and 0.99 ± 0.04 in EPO and PBS groups, respectively, $n = 6$ per group; $P < 0.05$) and locomotion (1.04 ± 0.04 and 0.85 ± 0.04 in EPO and PBS groups, respectively, $n = 6$ per group, $P < 0.05$). Mice showed rapid recovery from focal motor deficits and, by day 16 post-stroke, no motor deficits were detected based on a modified three-point scale (not shown).

Granulocyte colony-stimulating factor accelerates angiogenesis after stroke

Increased brain atrophy and impaired functional recovery in animals treated with G-CSF post-stroke were quite unexpected because of the known ability of G-CSF to mobilize CD34-positive cells from bone marrow (Willing et al., 2003). In addition, a previous study showed neuroprotective properties of G-CSF in models of transient cerebral ischemia (Schabitz et al., 2003). These considerations led us to analyse mechanisms contributing to increased brain atrophy after

TABLE 1. Raw data of open field test (G-CSF rearing)

Treatment and individual	Rearing (counts) Right ON	Right OFF	Reaction to darkness (Right OFF/Right ON)
PBS			
1	662	640	0.97
2	611	708	1.16
3	487	450	0.92
4	587	540	0.92
5	482	430	0.89
6	425	450	1.06
Mean ± SEM	542.3 ± 37.2	536.3 ± 47.1	0.99 ± 0.04
G-CSF (0.5µg/kg)			
1	600	562	0.94
2	601	650	1.08
3	494	425	0.86
4	731	731	1.00
5	767	784	1.02
6	498	501	1.01
Mean ± SEM	615.2 ± 46.7	608.8 ± 56.2	0.98 ± 0.03
G-CSF (5µg/kg)			
1	577	497	0.86
2	537	368	0.69
3	310	288	0.93
4	520	485	0.93
5	673	652	0.97
6	572	480	0.84
Mean ± SEM	531.5 ± 49.3	461.7 ± 50.8	0.87 ± 0.04
G-CSF (50µg/kg)			
1	592	520	0.88
2	463	376	0.81
3	478	430	0.90
4	307	250	0.81
5	484	410	0.85
6	385	295	0.77
Mean ± SEM	451.5 ± 39.6	380.2 ± 39.6	0.84 ± 0.02
G-CSF (250µg/kg)			
	578	424	0.73
	501	401	0.80
	507	380	0.75
	465	412	0.89
	380	341	0.90
	401	347	0.87
Mean ± SEM	472 ± 29.9	384.2 ± 14.0	0.82 ± 0.03

Right ON, under light condition; Right OFF, under dark condition.

administration of G-CSF. As G-CSF has been reported to accelerate angiogenesis in limb and cardiac models of ischemic injury (Minatoguchi et al., 2004), we sought to determine its impact on neovascularization in our permanent focal cerebral infarction model. Compared with PBS-treated controls (Fig. 2A), increased neovasculature at the border of the MCA and ACA cortex (staining with TTC demarcates viable/non-viable tissue and carbon black was used to visualize vessels) was observed in animals treated with G-CSF (50 µg/kg, Fig. 2B). Assessment of the angiographic score confirmed the impression of increased neovasculature in animals treated with G-CSF, compared with the group receiving PBS (Fig. 2C; $P < 0.05$).

Next, we investigated possible neuroprotective properties of G-CSF after stroke. Analysis of the infarcted/surviving area 3 days after stroke was evaluated in animals treated with PBS (Fig. 2D) or G-CSF (50 µg/kg, Fig. 2E) based on TTC staining; there was no effect of G-CSF treatment compared with controls receiving PBS (Fig. 2F). Thus, G-CSF did not impact on the viability of 'at-risk' tissue in the
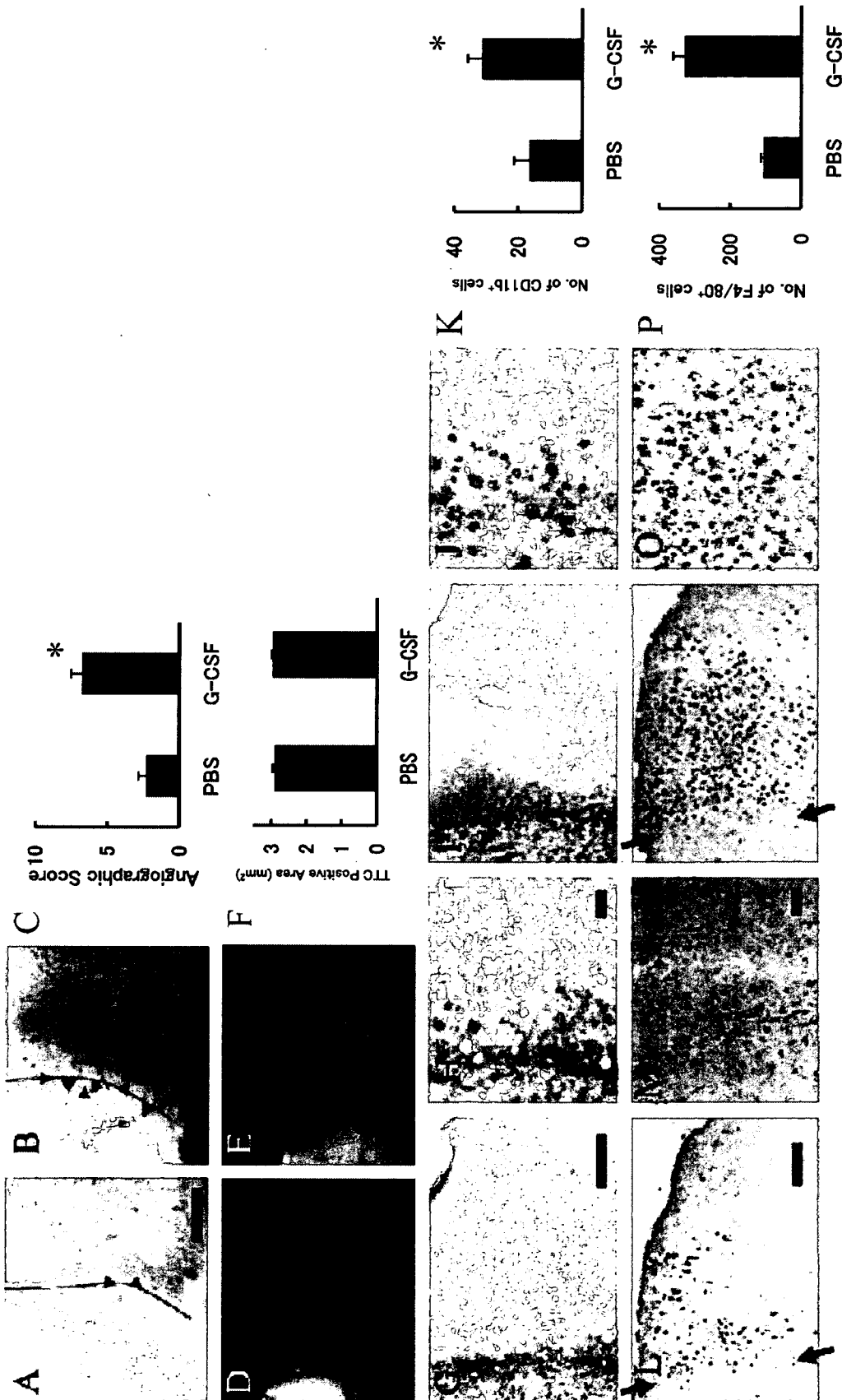
FIG. 2. Administration of granulocyte colony-stimulating factor (G-CSF) after stroke enhances the inflammatory response. (A–C) On day 3 after stroke, mice were infused with carbon black ink. Compared with mice treated with phosphate-buffered saline (PBS) (A), increased neovascularization was observed at the border between anterior cerebral artery (ACA) and middle cerebral artery (MCA) regions in mice treated with G-CSF (B). Representative micrographs are shown. The angiographic score (see Materials and methods) showed increased neovascularization ($n = 6$ per group) in mice treated with G-CSF post-stroke compared with controls (PBS). (D–F) There was no difference in the 2,3,5-triphenyltetrazolium (TTC)-positive ACA area at the exact center of forebrain comparing post-stroke animals treated with G-CSF (E) and controls/PBS (D). Sections from each animal were subjected to statistical analysis using Student's *t*-test ($n = 6$ animals per group; F). (G–K) CD11b-positive cells were visualized in the ACA area in tissue from post-stroke animals treated with PBS (G, lower magnification; H, higher magnification) or G-CSF (I, lower magnification; J, higher magnification). Sections from each animal were evaluated ($n = 6$ animals per group) and the average number of CD11b-positive cells per high power field is shown in each of the two groups (K). (L–P) F4/80-positive (F4/80⁺) activated macrophages/microglia in mice treated with PBS were relatively limited to the area close to the border of infarcted tissue (L, lower magnification; M, higher magnification). However, an expanded area and increased density of F4/80⁺ cells was observed after administration of G-CSF (N, lower magnification; O, higher magnification). The total number of F4/80⁺ activated macrophages/microglia in the viable ACA area identified on the section at exact center of forebrain was quantified ($n = 6$ per group) (N). Scale bars: 0.2 mm (A), 1 mm (D), 0.3 mm (G and L) and 30 μm (H and M). *$P < 0.05$ vs. PBS. Arrowheads (A and B) indicate microvessels at the border of the MCA and ACA cortex (red line). Arrows (L and N) indicate the border of infarcted tissue (left side, stroke MCA area; right side, viable ACA area).

immediate post-stroke period (up to 3 days), although there was a long-term effect on brain atrophy (evaluated at 35 days).

Granulocyte colony-stimulating factor enhances the inflammatory response after stroke

Further studies were performed to analyse the apparent dichotomy between G-CSF-mediated enhancement of neovascularization of the ischemic territory post-stroke vs. increased cerebral atrophy and lack of improvement in behavioral testing. We focused our studies on the inflammatory response. Compared with PBS-treated mice (Fig. 2G, lower magnification; Fig. 2H, higher magnification), increased accumulation of CD11b-positive inflammatory cells, including monocytes and granulocytes (Campanella et al., 2002), was observed in G-CSF-treated mice (50 µg/kg) at the border of the infarcted area (Fig. 2I, lower magnification; Fig. 2J, higher magnification). Quantitative analysis ($n = 6$ each) revealed a significant difference in the number of infiltrating CD-11b-positive cells (Fig. 2K; $P < 0.05$). These results led us to evaluate the presence of activated macrophages/microglia in ischemic lesions, as the latter are known to enhance brain damage after stroke (Mabuchi et al., 2000). Although F4/80[+] activated macrophages/microglia were observed in the viable (i.e. non-ischemic) ACA area following treatment with PBS (Fig. 2L, lower magnification; Fig. 2M, higher magnification), increased numbers of F4/80[+] macrophages/microglia were observed in post-stroke animals treated with G-CSF (Fig. 2N, lower magnification; Fig. 2O, higher magnification). F4/80[+] activated macrophages/microglia in post-stroke mice treated with PBS were principally limited to the area close to the border of the infarcted tissue. In contrast, F4/80^{+} cells in post-stroke mice treated with G-CSF were observed in a broad area and at higher density in the ACA territory. The total number of F4/80^{+} cells in a section at the exact center of the forebrain was quantified ($n = 6$ each); a significant increase in F4/80[+] activated macrophages/microglia was observed in G-CSF-treated mice, compared with controls receiving PBS post-stroke (Fig. 2P; $P < 0.05$).

Administration of granulocyte colony-stimulating factor 1 h after stroke also induces brain atrophy

As the experimental protocol for the above studies involved G-CSF treatment starting 24 h after stroke, it was important to vary our protocol. For this purpose, we also administered G-CSF within 1 h of stroke (Fig. 3A, $n = 6$ each) or performed continuous treatment for up to 7 days (Fig. 3B, $n = 6$ each). Our results demonstrate induction of brain atrophy in post-stroke animals treated with G-CSF subjected to either of these protocols compared with PBS-treated controls.

To exclude the immune response stimulated by human recombinant G-CSF in mice, various doses of mouse recombinant G-CSF were administered and the effect was determined ($n = 6$ each dose). We found significant brain atrophy with administration of lower doses (0.5 and 5 µg/kg) of recombinant murine G-CSF. As the survival rate was only 50% (three mice dead out of six) with administration of a higher dose (50 µg/kg), the group was excluded from this analysis.
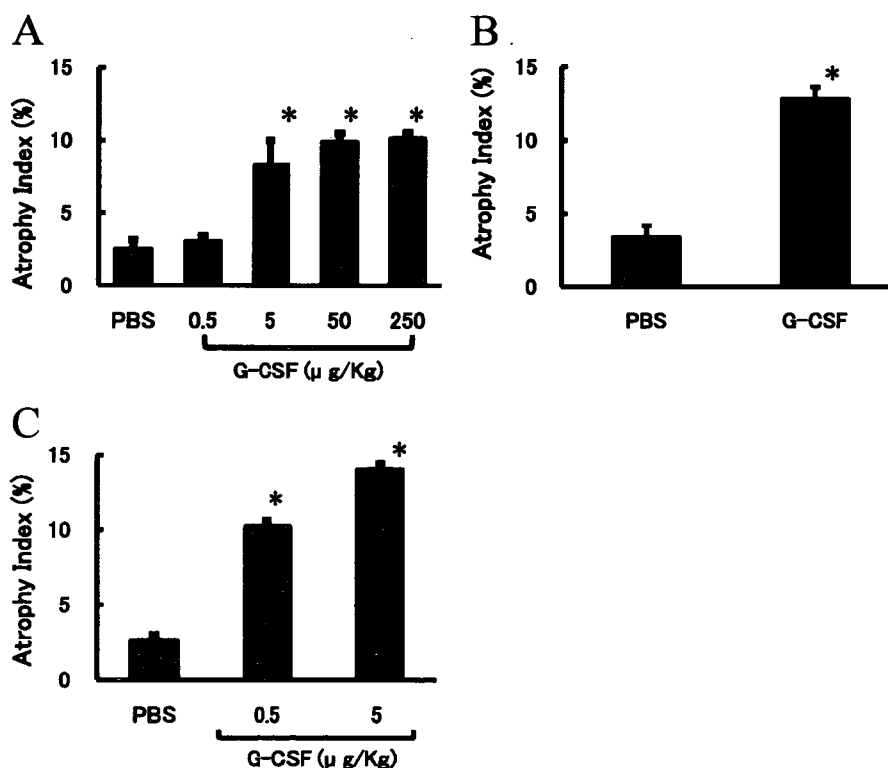
FIG. 3. Effect of granulocyte colony-stimulating factor (G-CSF) on brain atrophy. (A) G-CSF or phosphate-buffered saline (PBS) was administered 1 h after stroke and brains were evaluated grossly on day 35 post-stroke. (B) Continuous administration of G-CSF or PBS starting at 1 h post-stroke for 7 days was also tested. (C) Mouse recombinant G-CSF was administrated at the indicated dose and was found to increase the atrophy index. In each case, $n = 6$ per group. *$P < 0.05$ vs. PBS.

Discussion

Our results demonstrate that, in a murine permanent focal cerebral infarction model, administration of G-CSF, either human or murine recombinant, post-stroke is associated with enhanced brain atrophy.

In order to evaluate experimental treatments for stroke, reproducible induction of cerebral ischemia/infarction is a prerequisite. Previously, we developed a stroke model using SCID mice (Taguchi et al., 2004) that proved suitable for quantification of the effect of cell therapy on neurogenesis, neovessel formation and neural function. In the current study, we have applied this stroke model to CB-17 mice and found it to provide highly reproducible data.

Granulocyte colony-stimulating factor is known to mobilize EPCs from bone marrow (Willing et al., 2003) and accelerate angiogenesis (Bussolino et al., 1991). Clinical studies have demonstrated that administration of G-CSF has beneficial effects in patients with acute myocardial infarction, including promotion of neovascularization and improvement of perfusion (Kuethe et al., 2004). In addition, G-CSF has been shown to display neuroprotective properties in a rodent model (Schabitz et al., 2003). Based on these observations, G-CSF has been tested in animal models of transient cerebral ischemia and beneficial effects have been reported (i.e. reduced infarct volume and enhanced functional recovery) (Schabitz et al., 2003; Shyu et al., 2004; Gibson et al., 2005). In the current study, we employed a permanent cerebral infarction (i.e. stroke) model, rather than a model of transient ischemia, to investigate the effects of G-CSF.

In addition to its effects on EPCs, G-CSF is known to mobilize granuloctyes from the bone marrow, and these granulocytes have been shown to become associated with endothelia and accumulate in the ischemic brain (Justicia et al., 2003). These observations suggested the possibility that G-CSF might augment the inflammatory response consequent to ischemic tissue damage by promoting recruitment and activation of neutrophils and mononuclear-derived cells (blood monocytes, monocyte-derived macrophages and microglia) (Zawadzka & Kaminska, 2005). Consistent with this concept, accumulation of CD11b-positive inflammatory cells at the border of the infarcted area was observed after treatment with G-CSF. Furthermore, a striking increase in the number of F4/80$^+$ activated macrophages/microglia was observed in non-ischemic surviving tissue (adjacent to the infarct) subsequent to administration of G-CSF. The inflammatory response after stroke has been shown to have both positive and negative effects on tissue repair (Fontaine et al., 2002). Our results indicated that the balance of these inflammatory mechanisms on stroke outcome in the mouse using a permanent ischemia model and following administration of G-CSF is negative.

It would appear that the current work contradicts previous studies showing a positive effect of G-CSF after myocardial ischemia (Minatoguchi et al., 2004). This apparent discrepancy may be explained, at least in part, by differences in brain and cardiac vasculature. Non-ischemic brain is protected from the systemic inflammatory response by an intact blood–brain barrier composed of endothelia joined by tight junctions. Thus, invasion of the central nervous system by activated inflammatory cells is largely prevented and the neural system functions within a relatively protected microenvironment, with respect to the inflammatory response (Neumann, 2000). However, stroke disturbs the integrity of the blood–brain barrier. We propose that a combination of impaired function of the blood–brain barrier in the context of G-CSF-induced augmentation of the inflammatory response in ischemic tissue contributes to the observed brain atrophy. Although activated inflammatory cells are known to participate in both the injurious and healing processes (Minatoguchi et al., 2004), our results indicate an overall negative

effect on neural function and neurogenesis following treatment with G-CSF in the post-stroke period.

In contrast to G-CSF, EPO had beneficial effects after stroke in the current model. Such positive effects are consistent with previous reports (Bernaudin et al., 1999; Bahlmann et al., 2004; Bartesaghi et al., 2005; Kretz et al., 2005) demonstrating that EPO promotes mobilization of EPCs (Bahlmann et al., 2004), has angiogenic (Jaquet et al., 2002) and neuroprotective properties (Bartesaghi et al., 2005), and accelerates regeneration (Kretz et al., 2005).

Taken together, our results indicate that administration of G-CSF after stroke results in an exaggerated inflammatory response, both at the border of the ischemic region and also in non-ischemic brain tissue, and that this is associated with brain atrophy and poor neural function. Thus, we suggest that a cautious approach should be taken in applying results of studies with G-CSF in the peripheral circulation (i.e. limb and cardiac ischemia) to the setting of cerebral ischemia. In a more general context, it is possible that agents with pro-inflammatory properties will prove less useful as therapeutic agents in cerebral ischemia in view of the above observations.

Acknowledgements

Abbreviations

ACA, anterior cerebral artery; EPC, endothelial progenitor cell; EPO, erythropoietin; F4/80$^+$, F4/80-positive; G-CSF, granulocyte colony-stimulating factor; MCA, middle cerebral artery; PBS, phosphate-buffered saline; SCID, severe combined immunodeficient; TTC, 2,3,5-triphenyltetrazolium.

References

Asahara, T., Murohara, T., Sullivan, A., Silver, M., van der Zee, R., Li, T., Witzenbichler, B., Schatteman, G. & Isner, J.M. (1997) Isolation of putative progenitor endothelial cells for angiogenesis. *Science*, 275, 964–967.

Bahlmann, F.H., De Groot, K., Spandau, J.M., Landry, A.L., Hertel, B., Duckert, T., Boehm, S.M., Menne, J., Haller, H. & Fliser, D. (2004) Erythropoietin regulates endothelial progenitor cells. *Blood*, 103, 921–926.

Bartesaghi, S., Marinovich, M., Corsini, E., Galli, C.L. & Viviani, B. (2005) Erythropoietin: a novel neuroprotective cytokine. *Neurotoxicology*, 26, 923–928.

Bernaudin, M., Marti, H.H., Roussel, S., Divoux, D., Nouvelot, A., MacKenzie, E.T. & Petit, E. (1999) A potential role for erythropoietin in focal permanent cerebral ischemia in mice. *J. Cereb. Blood Flow Metab.*, 19, 643–651.

Bussolino, F., Ziche, M., Wang, J.M., Alessi, D., Morbidelli, L., Cremona, O., Bosia, A., Marchisio, P.C. & Mantovani, A. (1991) In vitro and in vivo activation of endothelial cells by colony-stimulating factors. *J. Clin. Invest.*, 87, 986–995.

Campanella, M., Sciorati, C., Tarozzo, G. & Beltramo, M. (2002) Flow cytometric analysis of inflammatory cells in ischemic rat brain. *Stroke*, 33, 586–592.

Dzau, V.J., Gnecchi, M., Pachori, A.S., Morello, F. & Melo, L.G. (2005) Therapeutic potential of endothelial progenitor cells in cardiovascular diseases. *Hypertension*, 46, 7–18.

Ehrenreich, H., Hasselblatt, M., Dembowski, C., Cepek, L., Lewczuk, P., Stiefel, M., Rustenbeck, H.H., Breiter, N., Jacob, S., Knerlich, F., Bohn, M., Poser, W., Ruther, E., Kochen, M., Gefeller, O., Gleiter, C., Wessel, T.C., De Ryck, M., Itri, L., Prange, H., Cerami, A., Brines, M. & Siren, A.L. (2002) Erythropoietin therapy for acute stroke is both safe and beneficial. *Mol. Med.*, 8, 495–505.

Fontaine, V., Mohand-Said, S., Hanoteau, N., Fuchs, C., Pfizenmaier, K. & Eisel, U. (2002) Neurodegenerative and neuroprotective effects of tumor

necrosis factor (TNF) in retinal ischemia: opposite roles of TNF receptor 1 and TNF receptor 2. *J. Neurosci.*, **22**, RC216.

Gibson, C.L., Bath, P.M. & Murphy, S.P. (2005) G-CSF reduces infarct volume and improves functional outcome after transient focal cerebral ischemia in mice. *J. Cereb. Blood Flow Metab.*, **25**, 431–439.

Jaquet, K., Krause, K., Tawakol-Khodai, M., Geidel, S. & Kuck, K.H. (2002) Erythropoietin and VEGF exhibit equal angiogenic potential. *Microvasc. Res.*, **64**, 326–333.

Justicia, C., Panes, J., Sole, S., Cervera, A., Deulofeu, R., Chamorro, A. & Planas, A.M. (2003) Neutrophil infiltration increases matrix metalloproteinase-9 in the ischemic brain after occlusion/reperfusion of the middle cerebral artery in rats. *J. Cereb. Blood Flow Metab.*, **23**, 1430–1440.

Kimble, D.P. (1968) Hippocampus and internal inhibition. *Psychol. Bull.*, **70**, 285–295.

Kretz, A., Happold, C.J., Marticke, J.K. & Isenmann, S. (2005) Erythropoietin promotes regeneration of adult CNS neurons via Jak2/Stat3 and PI3K/AKT pathway activation. *Mol. Cell Neurosci.*, **29**, 569–579.

Kuethe, F., Figulla, H.R., Voth, M., Richartz, B.M., Opfermann, T., Sayer, H.G., Krack, A., Fritzenwanger, M., Hoffken, K., Gottschild, D. & Werner, G.S. (2004) Mobilization of stem cells by granulocyte colony-stimulating factor for the regeneration of myocardial tissue after myocardial infarction. *Dtsch. Med. Wochenschr.*, **129**, 424–428.

Mabuchi, T., Kitagawa, K., Ohtsuki, T., Kuwabara, K., Yagita, Y., Yanagihara, T., Hori, M. & Matsumoto, M. (2000) Contribution of microglia/macrophages to expansion of infarction and response of oligodendrocytes after focal cerebral ischemia in rats. *Stroke*, **31**, 1735–1743.

Matsushita, K., Matsuyama, T., Nishimura, H., Takaoka, T., Kuwabara, K., Tsukamoto, Y., Sugita, M. & Ogawa, S. (1998) Marked, sustained expression of a novel 150-kDa oxygen-regulated stress protein, in severely ischemic mouse neurons. *Brain Res. Mol. Brain Res.*, **60**, 98–106.

Minatoguchi, S., Takemura, G., Chen, X.H., Wang, N., Uno, Y., Koda, M., Arai, M., Misao, Y., Lu, C., Suzuki, K., Goto, K., Komada, A., Takahashi, T., Kosai, K., Fujiwara, T. & Fujiwara, H. (2004) Acceleration of the healing process and myocardial regeneration may be important as a mechanism of improvement of cardiac function and remodeling by postinfarction granulocyte colony-stimulating factor treatment. *Circulation*, **109**, 2572–2580.

Neumann, H. (2000) The immunological microenvironment in the CNS: implications on neuronal cell death and survival. *J. Neural Transm. Suppl.*, **59**, 59–68.

Schabitz, W.R., Kollmar, R., Schwaninger, M., Juettler, E., Bardutzky, J., Scholzke, M.N., Sommer, C. & Schwab, S. (2003) Neuroprotective effect of granulocyte colony-stimulating factor after focal cerebral ischemia. *Stroke*, **34**, 745–751.

Shyu, W.C., Lin, S.Z., Yang, H.I., Tzeng, Y.S., Pang, C.Y., Yen, P.S. & Li, H. (2004) Functional recovery of stroke rats induced by granulocyte colony-stimulating factor-stimulated stem cells. *Circulation*, **110**, 1847–1854.

Taguchi, A., Soma, T., Tanaka, H., Kanda, T., Nishimura, H., Yoshikawa, H., Tsukamoto, Y., Iso, H., Fujimori, Y., Stern, D.M., Naritomi, H. & Matsuyama, T. (2004) Administration of CD34+ cells after stroke enhances neurogenesis via angiogenesis in a mouse model. *J. Clin. Invest.*, **114**, 330–338.

Tamatani, M., Matsuyama, T., Yamaguchi, A., Mitsuda, N., Tsukamoto, Y., Taniguchi, M., Che, Y.H., Ozawa, K., Hori, O., Nishimura, H., Yamashita, A., Okabe, M., Yanagi, H., Stern, D.M., Ogawa, S. & Tohyama, M. (2001) ORP150 protects against hypoxia/ischemia-induced neuronal death. *Nat. Med.*, **7**, 317–323.

Walther, T., Olah, L., Harms, C., Maul, B., Bader, M., Hortnagl, H., Schultheiss, H.P. & Mies, G. (2002) Ischemic injury in experimental stroke depends on angiotensin II. *Faseb J.*, **16**, 169–176.

Wang, L., Zhang, Z., Wang, Y., Zhang, R. & Chopp, M. (2004) Treatment of stroke with erythropoietin enhances neurogenesis and angiogenesis and improves neurological function in rats. *Stroke*, **35**, 1732–1737.

Weaver, C.H., Buckner, C.D., Longin, K., Appelbaum, F.R., Rowley, S., Lilleby, K., Miser, J., Storb, R., Hansen, J.A. & Bensinger, W. (1993) Syngeneic transplantation with peripheral blood mononuclear cells collected after the administration of recombinant human granulocyte colony-stimulating factor. *Blood*, **82**, 1981–1984.

Willing, A.E., Vendrame, M., Mallery, J., Cassady, C.J., Davis, C.D., Sanchez-Ramos, J. & Sanberg, P.R. (2003) Mobilized peripheral blood cells administered intravenously produce functional recovery in stroke. *Cell Transplant.*, **12**, 449–454.

Zawadzka, M. & Kaminska, B. (2005) A novel mechanism of FK506-mediated neuroprotection: downregulation of cytokine expression in glial cells. *Glia*, **49**, 36–51.

NDT
Nephrology Dialysis Transplantation

Original Article

Intrarenal administration of recombinant human soluble thrombomodulin ameliorates ischaemic acute renal failure

Takenori Ozaki[1], Chabouk Anas[1,2], Shoichi Maruyama[1], Tokunori Yamamoto[2], Kaoru Yasuda[1], Yoshiki Morita[1], Yasuhiko Ito[1], Momokazu Gotoh[2], Yukio Yuzawa[1] and Seiichi Matsuo[1]

[1]Department of Nephrology and [2]Department of Urology, Nagoya University Graduate School of Medicine, 65 Tsurumaicho, Showaku, Nagoya, Japan 466-8550, Japan

Abstract

Background. Thrombomodulin (TM) is an endothelial anti-coagulant cofactor which also has anti-inflammatory properties. The present study was performed to investigate the effects of recombinant human soluble TM (RHS-TM) on ischaemia/reperfusion (I/R) renal injury.

Methods. A right nephrectomy was performed in rats, and the left kidney was filled with RHS-TM (0.25 mg/kg), argatroban (20 mg/kg) or a vehicle for 45 min. Before reperfusion, the fluid trapped in the kidney was completely removed. At 24 h after I/R, renal cortical blood flow was measured using a CCD video camera, and the kidneys were harvested for the study. Next, cultured human umbilical vein endothelial cells were treated with RHS-TM (2, 10 or 50 mg/ml) or a vehicle, and incubated for 5 h in culture medium containing 300 μM hydrogen peroxide. Apoptotic cell death was analysed by terminal deoxynucleotidyl transferase dUTP nick-end labelling (TUNEL) assay.

Results. Immunohistochemistry revealed that the level of TM expression decreased in rat kidneys after I/R. RHS-TM significantly decreased blood urea nitrogen and serum creatinine levels. It also prevented a reduction in cortical blood flow, and attenuated tubular damage and macrophage/neutrophil infiltration. In addition, the number of TUNEL-positive cells decreased significantly in rats treated with RHS-TM. In contrast, argatroban, an inhibitor of thrombin did not show significant renoprotective actions. The results of *in vitro* study showed that RHS-TM significantly suppressed the number of apoptotic cells.

Conclusion. The transient intrarenal administration of RHS-TM, but not argatroban, to the kidney attenuates I/R renal injury. The present study suggests that RHS-TM would be a useful tool in preventing transplanted kidney damage or treating acute renal failure in the clinical setting.

Keywords: apoptosis; blood flow; endothelium; ischaemia; thrombomodulin

Introduction

Acute renal failure is a major clinical problem and the morbidity and mortality of affected patients remain high [1]. Ischaemia/reperfusion (I/R)-induced renal injury is an important cause of acute renal failure [2]. It occurs when renal perfusion is reduced during shock. It is also a significant complication of vascular surgery of the aorta or kidney [3]. Furthermore, I/R injury occurs in the allografts during the process of organ retrieval, storage and re-establishment of blood flow. It is a common cause of impaired or delayed graft function [4]. I/R injury is also known to be closely associated with increased acute rejection episodes and late allograft failure [5]. These problems are almost always observed in cadaveric renal allografts that have been subjected to warm or cold ischaemia, then reperfusion [4]. The unsatisfactory results from such transplants hamper efforts to enlarge the donor pool through the use of marginal donor organs [6]. Therefore, efforts to reduce damage to kidneys exposed to I/R-induced injury are essential.

Thrombomodulin (TM) is a widely expressed endothelial cell membrane-bound glycoprotein, which is known to form a high-affinity complex with thrombin and converts thrombin from a procoagulant to an anti-coagulant enzyme [7]. The thrombin–TM complex potently activates anti-coagulant protease protein C, thereby inhibiting thrombus formation [7,8]. TM is known to preserve the integrity of the endothelium. When endothelial cells are damaged, soluble TM is released into circulation [9,10]. Sido et al. [11] reported that the levels of soluble TM in the sera of patients who received liver transplant correlated

Correspondence to: Dr Shoichi Maruyama, MD, Department of Nephrology, Nagoya University Graduate School of Medicine, 65 Tsurumaicho, Showaku, Nagoya, Japan 466-8550, Japan.
Email: marus@med.nagoya-u.ac.jp

well with the degree of early graft damage. Soluble TM can be used as a marker of endothelial cell damage. Conversely, Salomaa *et al.* [12] demonstrated that a high plasma level of soluble TM in healthy people may protect the endothelial cells from injury and is associated with decreased risk of coronary heart disease.

Recombinant human TM (RHS-TM), a soluble derivative of human TM, has been produced [8]. Like native TM, RHS-TM binds directly to thrombin, and shows potent anti-coagulant activity [13]. RHS-TM is effective in animal models of disseminated intravascular coagulation [14–16]. Moreover, recent studies have shown that RHS-TM acts as a potent anti-inflammatory molecule in settings such as endotoxin-induced tissue damage [17] and atherothrombosis [18]. RHS-TM is also known to reduce liver damage following hepatectomy in cirrhotic rats, and suppresses I/R injury of the liver [19]. Concerning the kidney and RHS-TM, we have demonstrated that RHS-TM suppresses leucocyte/macrophage infiltration in the glomeruli and attenuated the renal damage in a rat model of thrombotic glomerulonephritis [20].

In our efforts to find a better way to protect the kidney from I/R injury, we hypothesized that soluble TM would be released from the endothelial cells of the kidney after I/R, and that the local administration of RHS-TM would ameliorate the renal injury by suppressing inflammation as well as by attenuating apoptosis. The purposes of the present study were to determine the therapeutic effects of RHS-TM on I/R renal injury and investigate the possible mechanisms involved.

Materials and methods

Animals

Male Sprague-Dawley rats weighing 250–300 g were purchased from Chubu Kagaku Shizai Co. Ltd (Nagoya, Japan) and were allowed free access to food and water. The protocols were approved by the Animal Care and Use Committee of Nagoya University, and the experiments were performed according to the Animal Experimentation Guidelines of Nagoya University Graduate School of Medicine.

Experimental protocols

Experiment 1

Six rats were anaesthetized by the intraperitoneal injection of sodium pentobarbital (50 mg/kg body weight) and a right nephrectomy was performed via flank incision. Seven days later, rats were anaesthetized again by the intraperitoneal injection of sodium pentobarbital, and the abdominal cavity was opened via midline incision. The viscera were placed aside and wrapped with wet gauze, the aorta and renal vessels (artery and veins) were exposed and isolated. The aorta

was clamped above the left renal artery first and then below. A 24-gauge cannula was placed in the aorta between the two clamps, and 2 ml of saline was administered slowly into the left kidney. Then, the renal artery and vein were clamped, the hole was covered with surgical glue and the original clamps were removed. Blood flow was restored after 45 min of ischaemia. The left kidneys were removed at 5 min ($n = 3$) and 18 h ($n = 3$) after reperfusion. Kidneys from three other normal rats served as controls.

Experiment 2

A right nephrectomy was performed in 24 rats. Seven days later, I/R renal injury was induced in a similar way as in Experiment 1. The left renal vein was clamped and a hole was made in the vein wall using a 23-gauge needle and RHS-TM (0.25 mg/kg) dissolved in 2 ml of saline ($n = 6$), argatroban (20 mg/kg) in 2 ml of saline ($n = 6$), or 2 ml saline only ($n = 6$) was injected slowly into the left kidney, forcing the blood out through the hole in the vein, until all the blood in the kidney had been drained. In order to ensure comparable anti-coagulant activities (elongation of APTT), appropriate dosages of each drug were determined based on information from a previous study [13]. All excess RHS-TM, argatroban, or saline which exited the vein hole was completely absorbed using a sponge on a stick. The renal artery and vein were clamped with a 10 mm micro-aneurysm clip (Mizuho Ikakogyo, Tokyo, Japan). The aorta hole was closed with surgical glue, and the two aorta clips were taken off, leaving the injected fluid trapped inside the kidney. After 45 min of ischaemia, another clamp was placed at the renal vein and the clip at the renal artery and vein was removed. The RHS-TM, argatroban, or saline trapped in the kidney during the ischaemic period came out of the vein hole, and the fluid was again completely wiped away. Then, the hole was closed by applying pressure for 5 min. Control rats ($n = 6$) underwent sham operation. At 24 h after reperfusion, RBC velocity in peritubular capillaries was measured using a pencil type CCD video microscope [21]. Rats were then sacrificed and blood and kidney samples were collected for the study. Normal rats ($n = 4$) were also used to obtain the baseline data of renal cortical microcirculation.

Direct vision using a CCD video microscope

An intravital CCD video microscope which has a pencil lens probe with a tip diameter of 1 mm was used in this study. The probe has a magnification of ×520 and spatial resolution of 0.86 μm, permitting identification of individual blood cells [21,22]. This device enabled us to get a direct image of microcirculation in various organs in humans as well as organs in large and small animals, including pigs, rabbits, rats and mice. The blood flow in renal CTC was observed, and the images were recorded using the freeze-frame mode.

The speed of RBCs in individual segments of the CTC was analysed using a point tracking method and motion detection program.

Coagulation parameters, serum creatinine and blood urea nitrogen

Two millilitre of blood was transferred into a plastic syringe containing 0.22 ml of 3.8% trisodium citrate, and plasma was prepared by centrifugation at 1710 g for 10 min. Prothrombin time (PT) and activated partial prothrombin time (APTT) were measured by Mitsubishi BCL Co. Ltd (Tokyo, Japan). The rest of the blood was collected into a glass tube, stored overnight and centrifuged at 1500 r.p.m. for 10 min. Serum creatinine and blood urea nitrogen (BUN) were measured using Daiya Auto UN or Daiya Auto Crea Kit (Daiya Shiyaku, Tokyo, Japan).

Histology and immunohistochemistry

One part of the kidney was fixed with 4% paraformaldehyde, embedded in paraffin, and cut into 4 μm sections. These were stained with haematoxylin and eosin (HE) and periodic acid-Schiff reagent (PAS). Another part of the kidney was frozen in OCT compound (Miles, Elkhart, IN). Sections (2 μm thick) were fixed in acetone. Immunostaining was performed as previously described [23]. TM was stained with rabbit anti-rat TM Ab [24], followed by a fluorescein conjugate of goat anti-rabbit IgG Ab (Zymed Laboratories, San Francisco, CA). Monocytes/macrophages were stained with a fluorescein conjugate of mouse anti-rabbit ED1 Ab (Serotec, Raleigh, NC).

Morphometric analysis of histology and immunohistochemistry

To assess tubulointerstitial injury, PAS stained kidney sections were analysed using a semiquantitative grading as described previously [25] with minor modification. Briefly, the extent of tubular cast formation and tubular damage (dilatation and degeneration) in 16 non-overlapping fields (×200) of the outer medulla was scored according to the following criteria: 0, normal; 1, less than 10%; 2, 11–25%; 3, 26–45%; 4, 46–75% and 5, more than 76% of the pertinent area. Macrophage infiltration was assessed by counting the ED-1-positive cells in 16 non-overlapping fields (×400) of the outer medulla on frozen sections, and the numbers were expressed per field. Neutrophil infiltration was also evaluated using the HE sections in a similar way. The morphologic analysis was carried out by two observers in a blind fashion, using a Zeiss microscope (Oberkochen, Germany).

To evaluate the vascular density, kidney sections stained for rat TM were analysed. Photographs of six non-overlapping fields (×200) in the outer medulla were taken, and the areas positively stained for rat TM were measured using the MetaMorph 6.3 image

analysis computer program (Universal Imaging Co., West Chester, PA) [26].

Experiment 3

Dose dependency was studied using the same protocol as in Experiment 2. Right nephrectomy was performed on 20 rats. Seven days later, 2 ml of saline, or two different doses (0.025 and 0.25 mg/kg) of RHS-TM dissolved in 2 ml of saline (each $n = 5$) was injected into the left kidney. After 45 min of ischaemia, all kidneys were completely cleared of the administered reagents. Five rats were subjected to sham operation. At 24 h, rats were sacrificed and blood samples were collected for the study.

In vitro experimental design

Human umbilical vein endothelial cells (HUVECs) (Takara, Ootsu, Japan) were cultured in endothelial cell basal medium-2 (EBM-2) supplemented with 100 U/ml penicillin, 100 μg/ml streptomycin and an EGM-2 using the EGM-2 BulletKit (Takara). HUVECs were grown up to 90–95% confluence on four-well chamber slides (Nalge Nunc International, Rochester, NY), and cytoprotective effects of THS-TM were studied as described [27]. RHS-TM in doses of 2, 10 or 50 mg/ml, or saline was added to HUVECs in culture, and then incubated with 300 μM hydrogen peroxide for 5 h. Following incubation, apoptotic cell death was analysed by terminal deoxynucleotidyl transferase (TdT)-mediated dUTP nick-end labelling (TUNEL) assay.

TUNEL assay

Apoptotic cell death was determined on paraffin-embedded kidney sections (4 μm-thick) or HUVECs fixed in 4% paraformaldehyde by TUNEL staining using in situ Apoptosis Detection Kit (Takara) as described [27]. Six non-overlapping fields (×200) in the outer medulla of the kidney sections, and six non-overlapping fields (×200) on the cell culture chamber slides were photographed. The numbers of TUNEL-positive cells were counted using MetaMorph 6.3 (Universal Imaging Co.).

Statistical analyses

Statistical analysis was performed using a software program, Stat View 5.0 (SAS Institute, Cary, NC, USA). Two-way analysis of variance (ANOVA) was used to determine the significant difference among three groups. When statistical difference was indicated by ANOVA, further analysis was performed using Scheffe to determine the difference between any pair of groups. A significant difference was defined as a P-value of <0.05. All values are provided as mean $\pm$ SD.